BMC Microbiology

RESEARCH

Open Access

Prophylactic administration of overproducing-abscisic acid *Bacillus licheniformis* attenuated DSS-induced colitis in mice by regulating the gut microbiota and immune activity

Zeyan Xu[1], Lijiang Zhao[1], Mengting Wu[1], Anqi Cui[1], Wei Chen[1], Guohao Zheng[1], Jingyi Zhou[1], Daqing Gao[1*†] and Ruihua Shi[1,2*†]

Abstract

Background Inflammatory bowel disease (IBD) involves the complex interplay among the mucosal barrier, microbiota, immunity and genetic factors. There are currently no satisfactory treatments for IBD. Administration of the probiotic *Bacillus licheniformis* (Bl) can improves colitis by regulating the gut microbiota. The phytohormone abscisic acid (ABA) treatment has favorable effects on immunity, as well as on inflammatory diseases like colitis. We hypothesized that the expression of an additional *cyp* gene by the Bl to increase its ABA production would enhance its effects.

Results In this study, we found that a Bl-cyp strain overexpressing the *cyp* gene secreted more ABA into its supernatant than either the parental Bl stain or a Bl-pET82a strain expressing only a vector pET82a when these bacteria were grown in Nfb medium for 48 h. The prophylactic administration of the Bl-cyp strain culture more effectively attenuated dextran sodium sulfate (DSS)-induced colitis in mice compared to the Bl and Bl-pET28a strains. These findings were associated with significantly reduced epithelial barrier damage, as well as increased number of goblet cells and expression levels of *occludin* gene in the colonic epithelial layer, and decreased serum LPS levels in the Bl-cyp group. In addition, the administration of Bl-cyp strain effectively regulated the disordered gut microbiota by improving their diversity, richness and compositions more than the Bl or Bl-pET82a strain, including the ratio of *Bacteroidota*: *Bacillota*. It also inhibited the excessive growth of opportunistic pathogen *Escherichia* just like the Bl or Bl-pET82a strain. Moreover, the preventive administration of the Bl-cyp strain to mice following DSS-induced colitis enhanced the proportion of Treg cells and suppressed the proportion of Th17 cells in mesenteric lymph nodes (MLNs), decreased the levels of pro-inflammatory cytokines TNF-α, IL-6, and IL-22, and increased the level of

†Daqing Gao and Ruihua Shi contributed equally to this work.

*Correspondence:
Daqing Gao
dgao2@seu.edu.cn
Ruihua Shi
shiruihua@seu.edu.cn

Full list of author information is available at the end of the article

anti-inflammatory IL-10 in colon tissues, similar to treatment with a high concentration of the ABA standard (ABA-H). Notably, the treatment with the Bl-cyp strain more effectively regulated the disordered microbiota than the ABA-H.

Conclusions The administration of the Bl-cyp strain may provide a novel preventive approach for IBD, and may exert its effects by modulating the gut microbiota and host's immune status.

Keywords *Cyp* gene, Abscisic acid, *Bacillus licheniformis*, Inflammatory bowel disease, Gut microbiota

Background

Inflammatory bowel disease (IBD), including Crohn's disease (CD) and ulcerative colitis (UC), is associated with an imbalance of immunity, disordered gut microbiota, damage to the mucosal barrier and genetic factors [1]. IBD is an important disease worldwide, and is associated with frequent relapses [2]. Its incidence rate has been increasing yearly, and there are currently no satisfactory treatments [3].

The gut microbiota is composed of a cluster of microbes (mainly bacteria) present in the intestinal tract. These bacteria participate in many physiological and biochemical processes in the host, such as digestion [4], immune regulation [5] and short-chain fatty acids (SCFAs) metabolism [6]. Therefore, disorders of the microbiota not only lead to alterations in the intestinal epithelium, but also cause inflammation and contribute to triggering and/or aggravating IBD [7, 8]. Probiotics (which can alter the gut flora) have been demonstrated to provide positive effects against IBD [9].

Bacillus licheniformis (Bl) is a Gram-positive obligate aerobe that forms spore. It is a dominant population within soil and plant microbiota [10], but is not an inherent population in human and animal gut microbiota [11]. It was previously demonstrated that Bl could produce high levels of branched SCFAs (isobutyric acid and isovaleric acid) in the colon to regulate the gut microbiota [12]. Bl has been used as a live bacterial preparation to treat mice with colitis induced by dextran sodium sulfate (DSS) [13], human patients with subhealth [12], and human patients with acute and chronic diarrhea and ulcerative colitis [14]. It has proven safety and clinical effectiveness [14]. In addition, the Rt4M10 strain of Bl isolated from the roots of grapevines has been reported to produce abscisic acid (ABA) to diminish plant water losses, providing another potential mechanism of action underlying the benefits of these bacteria [15].

Abscisic acid (ABA) is a secondary metabolic and sesquiterpene product [16], which can function as a signaling molecule in a wide range of organisms, from bacteria to human cells, at a very low concentration [17, 18]. The best-known roles of ABA, which are synthesized by bacteria [15, 19], are in regulating plant growth and stress responses, leading to it being widely used in agriculture as a phytohormone [20]. In humans and animals, nutrient-derived ABA or treatment with synthetic ABA has been shown to produce favorable effects on immunity, as well as on inflammatory and metabolic diseases like colitis [21, 22]. ABA regulates adhesion molecule expression through a peroxisome proliferator activated receptor (PPAR) γ-dependent mechanism, resulting in activity against experimental IBD [23]. The PPARγ protein is a nuclear receptor expressed in epithelial and immune cells that regulates the differentiation of T helper 17 (Th17) cells and regulatory T (Treg) cells [24]. The differentiation of Th17 and Treg cells is also regulated by gut microbiota [25]. Th17 and Treg cells are both present in the intestinal mucosa, where they inhibit excessive immune responses and protect against pathogen invasion [26]. Some bacteria (*Klebsiella pneumonia* and *Proteus mirabilis*) found in the animal gut generate ABA, and the ABA content in an organism is very low [18, 27]. However, little has been reported about the roles of bacteria-generated ABA plays in the gut.

As indicated above, bacteria such as Bl [13] and fungi [28] can produce the ABA under certain conditions. The *bcaba1* gene encodes a cytochrome P450 monooxygenase and is associated with ABA biosynthesis in a fungus, *Botrytis cinerea* (*B.cinerea*) [28]. According to GenBank data, the sequence of a *cyp* gene encoding a cytochrome (cyp) P450 enzyme in the Bl strain (GenBank accession number: NC_006270) is highly homologous to that of the *bcaba1* gene in *B. cinerea.*

In this study, we developed a Bl-cyp strain that overexpresses this *cyp* gene to enhance its ABA production. We then explored whether the Bl-cyp strain could ameliorate the symptoms of mice with DSS-induced colitis. Our present study provides evidence that the Bl-cyp may be useful for the prevention of IBD.

Results

Identification of ABA from the supernatants of the Bl-cyp strain grown in Nfb medium

We first quantified the ABA from the supernatants of the Bl-cyp strain grown in Nitrogen -free (Nfb) medium. We cloned the *cyp* gene from the Bl ATCC 12,759 strain into a pET28a vector, and produced a recombinant pET82a-cyp in *E.coli* BL21. Under different induction condition, we found that the expression levels of the Cyp protein of pET82a-cyp/BL21 was higher than that of control pET82a/BL21 or BL21 when the bacteria in logarithmic growth phase were incubated at 37 °C for 4 h with

0.1 mmoL isopropyl-beta-d- thiogalacto-pyranoside (IPTG, Sigma-Aldrich, Germany) (Fig. 1a; Fig. S1-5). The transcriptional levels of the *cyp* gene in the Bl-cyp strain were also significantly higher than those in the Bl strain ($P < 0.001$), and the Bl-pET28a (vector-only) strain (Fig. 1b; $P < 0.001$).

Next, we investigated the conditions of ABA secretion into the medium by the Bl strain. In the 50 ppm ion traces, an ABA standard was seen at 4.54 min (Fig. 1c), and the ABA in the supernatant of the Bl strain grown in Nfb medium was detected at 5.12 min (Fig. 1d). It was not detected in Luria-Bertani (LB) medium according to the typical chromatography (Fig. 1e). We then compared the ABA standard with the supernatant of the Bl grown in Nfb medium using mass spectrometry. The results showed that the ABA in the supernatant was eluted on the 50-ppm ion trace at m/z 263 (Fig. 1f), which was the same as the molecular ion from the ABA standard (Fig. 1g). Finally, comparison of the ABA concentrations in the supernatants of the Bl strain grown in Nfb medium with those of the Bl-cyp or Bl-pET28a strain grown in the same medium for different times revealed that the concentrations of the Bl-cyp strain were higher than those of the Bl and Bl-pET28a strains from 48 to 72 h ($P < 0.001$; $P < 0.001$). The concentrations of ABA from of the Bl, Bl-pET28a and Bl-cyp strains were 26.5, 26 and 95 μg/mL, respectively, at 48 h (Fig. 1h). Thus, these strains could all secrete ABA into their culture media when grown on Nfb medium for 48 h, but the Bl-cyp produced the highest concentration.

Prophylactic administration of the Bl-cyp strain more effectively attenuated DSS -induced colitis in mice than the Bl or Bl-pET28a strain

Given their production of ABA and the beneficial effects of ABA on IBD, we investigated whether the prophylactic administration of the Bl strain culture (in Nfb) could reduce DSS-induced colitis in mice (Fig. 2a). As expected, the body weights in the control group mice were steady, and their disease activity index scores (DAIs; body weight loss, rectal bleeding and diarrhea) were zero. Compared with the control group, there were body weights loss and increased DAIs observed in the other groups beginning the day after DSS was added to the drinking water ($P < 0.001$). However, the weights loss and increase in the DAIs of the Bl group were significantly lower than those in the DSS and Nfb (blank media) groups (both $P < 0.001$), and there were no significant differences between the DSS and Nfb groups (Fig. 2b, c; $P = 0.2806$, $P = 0.6222$). The colon lengths, which were used to evaluate the severity of inflammation were shorter in the DSS group than in the control and Bl groups ($P < 0.001$ and $P = 0.006$), but were not significantly different from the Nfb group (Fig. 2d, e; $P = 0.137$).

Since some reports suggested that the Bl strain reduced the production of pro-inflammatory IL-6 in porcine intestinal epithelial cells [29], we observed the histological structures and measured the mRNA levels of the IL-6 gene in the mice with DSS-induced colitis. We found that the IL-6 levels in the colon tissue of the DSS group, were significantly higher than those in the control and Bl groups ($P < 0.001$; $P = 0.003$, respectively), but were not significantly different from the Nfb group (Fig. 2f; $P = 0.672$). The H&E-stained colon tissues in the DSS and Nfb groups revealed the strong erosion of the epithelial barrier, damaged of crypts, and apparent infiltration of inflammatory cells and ulceration, while normal colon structures were observed in the control group (Fig. 2g). The colon injury and inflammation in the Bl group were significantly reduced compared to the DSS group ($P = 0.007$), while those in the Nfb group were not significantly different from those in the DSS group (Fig. 2h; $P = 0.336$). The cumulative scores for each group were compared, and the results (Fig. 2h) were consistent with those shown in Fig. 2g. On the whole, these results demonstrated that DSS induced acute colitis in the mice, and that the prophylactic administration of the culture of the Bl strain, but not blank Nfb medium, could suppress the symptoms of colitis, and decrease inflammation in the colon tissues administered DSS.

Next, we investigated the effect of the Bl-cyp administration in the mice with DSS-induced colitis. Notably, the weights loss and increasing DAIs in the Bl-cyp group, were significantly lower than those in the Bl ($P < 0.001$; $P = 0.0491$) and Bl-pET28a groups (Fig. 2b, c; both $P < 0.001$). The colon lengths in the Bl-pET28a and Bl groups were significantly shorter than those in the Bl-cyp group (Fig. 2d, e; all $P < 0.001$). The transcriptional levels of the IL-6 gene in the colon tissue of the Bl-cyp group were significantly lower than those in the Bl-pET28a and Bl groups (Fig. 2f; all $P < 0.001$). In addition, the colon injury and inflammation in the Bl-cyp group were significantly reduced compared with the Bl-pET28a and Bl groups (Fig. 2g, h; all $P < 0.001$). On the whole, these results demonstrated that the prophylactic administration of the Bl-cyp strain culture more effectively decreased DSS-induced colitis than administration of the Bl-pET28a or Bl strain culture.

The Bl-cyp strain more effectively reinforced the epithelial barrier than the Bl or Bl-pET28a strain

To assess how these effects were occurring, we first examined the effects of the Bl administration on the epithelial barrier in mice with DSS-induced colitis. The mucus layer is on the surface of the epithelial cells in the gut. The mucus and and mucins are secreted by goblet cells, and enterocytes provide the first defense barrier in the intestinal tract [30]. Lipopolysaccharide (LPS) is an important

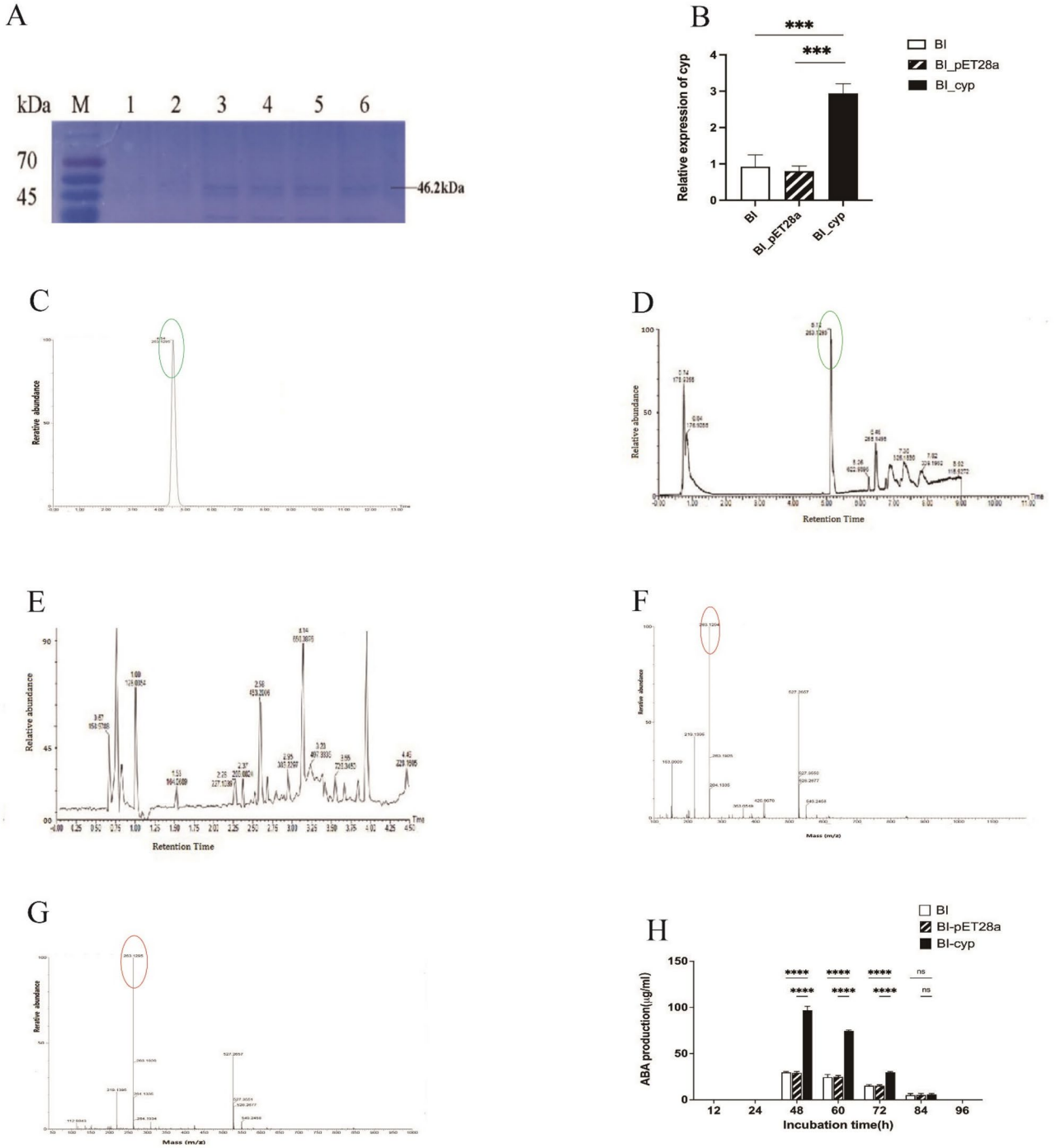

Fig. 1 Identification of ABA from the supernatant of the Bl or Bl-cyp strain grown on Nfb. **a** Comparison of the Cyp expression in pET28a-cyp/BL21, BL21, and pET28a/BL21 cultured with different concentrations of IPTG in LB at 37 °C for 4 h, as shown by SDS-PAGE. M represents the protein marker, 1–2 represent the BL21 and pET28a/BL21 cultured with 0.1 mM IPTG in LB; and 3–6 represent pET28a-cyp/BL21 cultured with 0.1, 0.2, 0.3 or 0.4 mM IPTG in LB, respectively. **b** Comparison of the mRNA expression of the *cyp* gene in the Bl and Bl-pET28a strains with that in the Bl-cyp strain grown in Nfb medium based on qRT-PCR. **c-d** Detection of the ABA from the ABA standard solution (**c**) and the supernatant of the Bl grown on Nfb (**d**) or LB medium (**e**) by typical chromatography. The green circles represent the ABA at 4.54 min and at 5.12 min. **f-g** Detection of ABA from the supernatants of the Bl grown in Nfb medium (**f**) and an ABA standard solution (**g**) based on typical mass spectrometry. The red circles indicate the ABA on the 50-ppm ion trace at m/z 263. **h** Comparison of the ABA concentrations on the supernatants from the Bl-cyp strain with those from the Bl and Bl-pET28a strains grown in Nfb at the different times according to ELISA. Data represent the means ± SD, $n = 6–8$ per group. *$P < 0.05$, ** $P < 0.01$; NS, not significant. Statistical significance was assessed using a one-way ANOVA, followed by Tukey's test

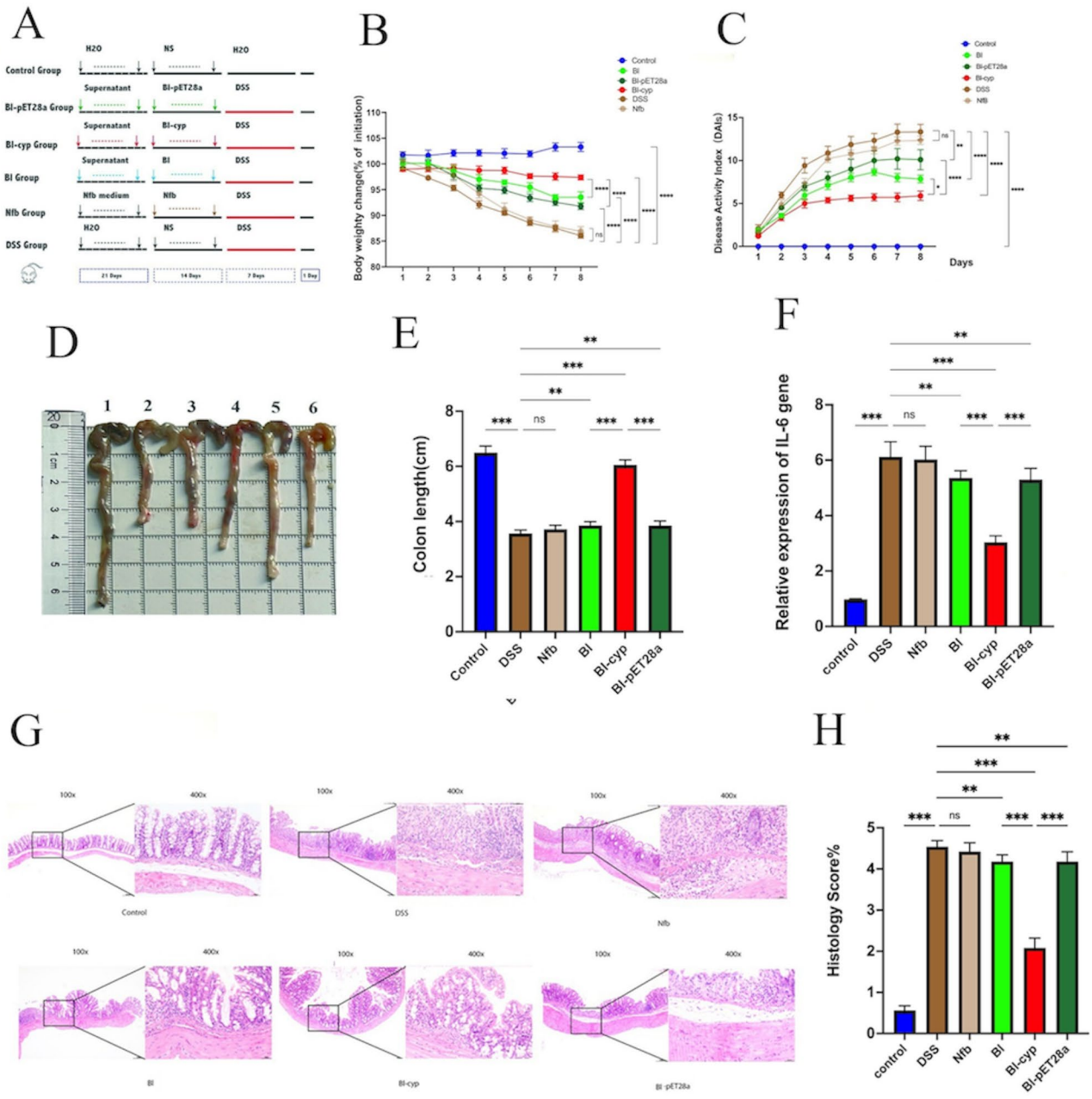

Fig. 2 Prophylactic administration of the Bl-cyp strain more effectively attenuated DSS-induced colitis. **a** Mice in the control, Bl-pET28a, Bl-cyp, Bl, Nfb and DSS groups with experimentally-induced colitis. **b** The body weights were recorded in the six groups beginning the day after DSS was added to the drinking water. **c** The DAIs were recorded in the six groups beginning the day after DSS was added to the drinking water, with scores based on body weight loss, rectal bleeding and diarrhea. **d** The entire colons in the six groups were harvested on Day 43. The numbers 1–6 represent the colon lengths in the control, DSS, Nfb, Bl, Bl-cyp and Bl-pET28a groups, respectively. **e** Comparison of the colon lengths in the DSS group with those in the control, Bl-cyp, Nfb, Bl and Bl-pET28a groups, and comparison of those in the Bl-cyp with those in the Bl and Bl-pET28a groups. **f** Comparison of the IL-6 mRNA expression in the colon tissues of the DSS group with those in the control, Nfb, Bl-pET28a, Bl-cyp and Bl groups, and comparison of those in the Bl-cyp group with those in the Bl-pET28a and Bl groups. **g** Representative pictures of the H&E-stained colon tissues from the six groups (scale bars, 100 μm; magnification, 100x or 400x). **h** Comparison of the cumulative histology scores of the colon tissues in the DSS group with those in the control, Nfb, Bl-pET28a, Bl-cyp and Bl groups, and comparison of those in the Bl-cyp group with those in the Bl-pET28a and Bl groups. Data represent the means ± SD, $n = 6–8$ per group, $^{*}P < 0.05$, $^{**}P < 0.01$, $^{***}P < 0.001$; NS, not significant. Statistical significance was assessed using a one-way ANOVA, followed by Tukey's test

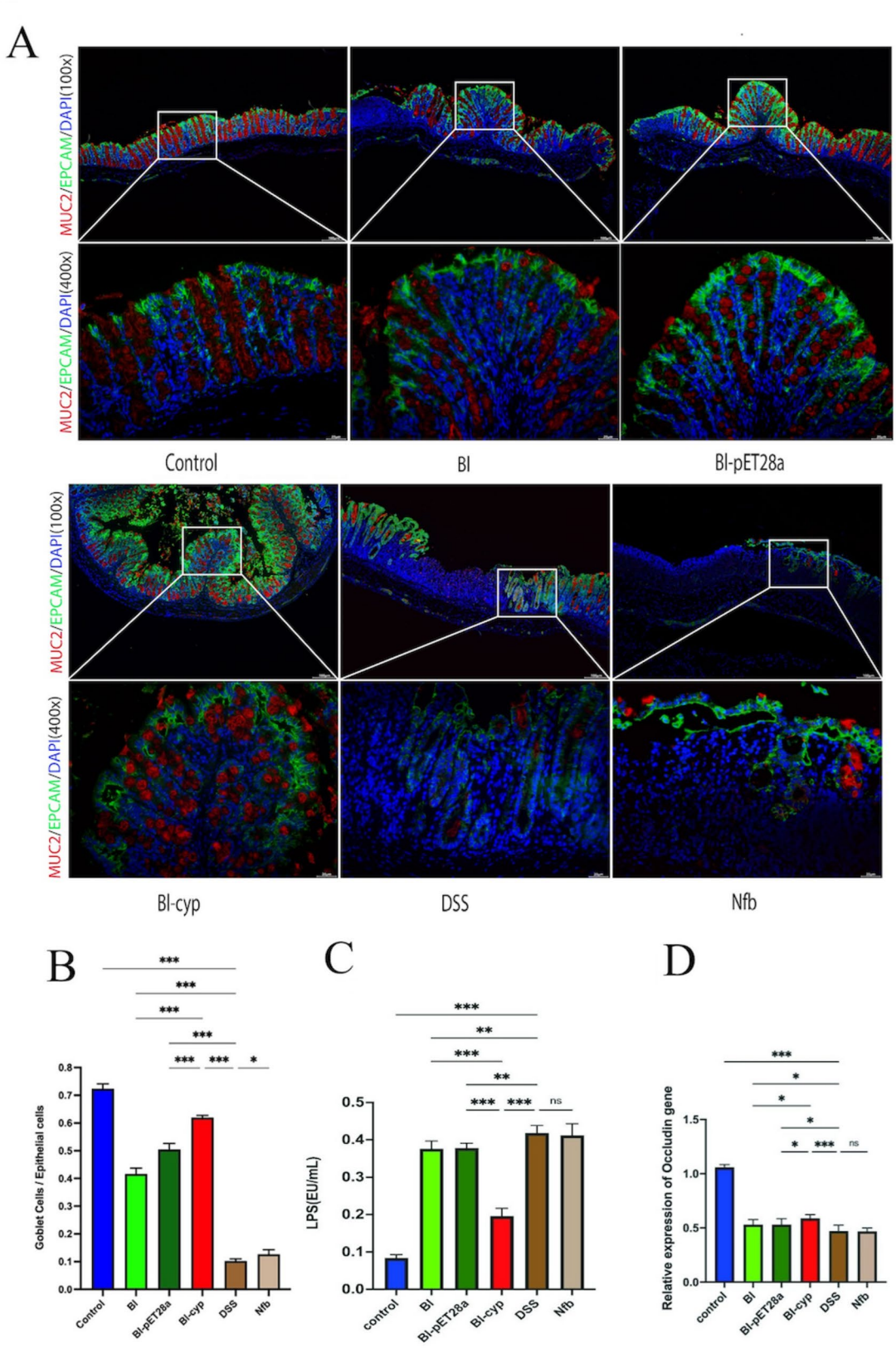

Fig. 3 (See legend on next page.)

(See figure on previous page.)

Fig. 3 Prophylactic administration of the Bl-cyp strain more effectively decreased DSS-induced epithelial barrier damage than other treatments. **a** Representative pictures of the goblet cells and epithelial cells in colonic epithelial layer from the control, Bl, Bl-pET28a, Bl-cyp, DSS and Nfb groups after immunofluorescence staining (scale bars,100 μm; magnification, 100x or 400x). The epithelial cell markers-EpCAM and CD326 appeared green and the goblet cell marker, MUC2 was red, and the cell nuclei stained by DAPI was blue. **b** Comparison of the proportion of goblet cells to epithelial cells in the DSS group with those in the control, Nfb, Bl, Bl-cyp and Bl-pET28a groups, and comparison of the proportion in the Bl-cyp group with those in the Bl-pET28a and Bl groups. **c** Comparison of the serum LPS levels in the DSS group with those in the control, Nfb, Bl, Bl-cyp and Bl-pET28a groups, and comparison of those in the Bl-cyp group with those in the Bl-pET28a and Bl groups. **d** Comparison of the mRNA expression of the *occludin* gene in the colon tissues of the DSS group with those in the control, Nfb, Bl, Bl-cyp and Bl-pET28a groups, and comparison of those in the Bl-cyp group with those in the Bl-pET28a and Bl group. Data represent the means ± SD, $n = 6–8$ per group. * $P < 0.05$, ** $P < 0.01$, *** $P < 0.001$; NS, not significant. Statistical significance was assessed using a one-way ANOVA, followed by Tukey's test

component of the cell walls in Gram -negative bacteria in the gut. The translocation of Gram-negative bacteria past the mucus and enterocytes therefore increases the serum level of LPS. As such, the LPS levels indicate the degree of permeability of the epithelial barrier [31]. A Occludin is a critical component of tight junctions in the gut epithelial barrier [32]. The LPS levels in the serum, the expression of the *occludin* gene and the numbers of goblet cells in the gut epithelium all reflect the extent of the epithelial barrier damage in the gut. We observed that the numbers of goblet cells in colonic epithelial layer of the DSS group were significantly lower than those in the control, Bl and Nfb groups (Fig. 3a, b; $P < 0.001$, $P < 0.001$, $P = 0.015$). The LPS levels in the sera of the DSS group were significantly increased compared to those in the control and Bl groups ($P < 0.001$ and $P = 0.003$), but not compared to the Nfb group (Fig. 3c; $P = 0.646$). Similarly, the levels of *occludin* gene expression in the DSS group were significantly lower than those in the control and Bl groups ($P < 0.001$; $P = 0.039$), but not in the Nfb group (Fig. 3d; $P = 0.942$). Therefore, these results show that the administration of Bl strain culture reinforced the epithelial barrier and attenuated DSS-induced damage, while the Nfb medium alone did not.

Next, we examined the effects of the Bl-cyp strain on DSS-induced epithelial barrier damage. Compared to the Bl-pET28a and Bl groups, the numbers of goblet cells in colonic epithelial layer of the Bl-cyp group were significantly increased (Fig. 3a, b; all $P < 0.001$), and the LPS levels in the sera were significantly decreased (Fig. 3c; all $P < 0.001$). The levels of *occludin* gene expression in the colon tissues in the Bl-cyp group were significantly higher than those in the Bl-pET28a and Bl groups (Fig. 3d; all $P = 0.039$). Thus, the prophylactic administration of the Bl-cyp strain culture more efficiently reinforced the epithelial barrier and attenuated DSS-induced damage than the Bl or Bl-pET28a strain culture.

The Bl-cyp strain more effectively modulated gut microbiota than the Bl or Bl -pET28a strain

Examined the impact of Bl administration on the gut microbiota in mice with DSS-induced colitis. The α-diversity represents the richness and evenness of microbial communities in an ecological system. Compared with the DSS group, the α-diversity of microbial communities in the control and Bl groups significantly increased (all $P < 0.001$), but that in the DSS group was not significantly different from that in the Nfb group based on the amplicon sequence variants (ASVs) level of the Sobs index (Fig. 4a; $P = 0.773$). A barplot analysis was performed to assess the microbial compositions at the phylum and genus levels, and there were the different abundances of the compositions in the six groups (Fig. 4c, d). To define the changes in the taxonomic composition of the gut microbiota in the Bl group, we performed a linear discriminant analysis (LDA; scores > 3.6) to identify differentially abundant biomarkers from the phylum to genus levels between the DSS and Bl groups (Fig. 4b). The results showed that the DSS group was more enriched in *Bacteroides*, *Enterobacteriaceae* and *Escherichia* than the Bl group. Therefore, these results showed that prophylactic administration of the Bl strain culture decreased the disorder of DSS-induced gut microbiota and reduced the abundances of conditioned pathogens in the gut.

Next, we explored the impact of the Bl-cyp strain on the gut microbiota in the mice with DSS-induced colitis. Compared with the Bl-cyp group, α-diversity in the Bl-pET28a and Bl groups were significantly decreased based on the ASV levels of the Sobs index (Fig. 4a; $P = 0.043$; $P = 0.047$, respectively). The β-diversity indicates the relationships between ecological systems. A principle components analysis (PCoA) showed clear separations among the gut microbiota in the control, Bl-cyp, Bl-pET28a, Bl, Nfb and DSS groups (Fig. 4e; $R^2 = 0.7594$; $P = 0.0001$). These results revealed that the gut microbiota in the Bl-cyp and control groups were obvious different from those in the DSS, Nfb, Bl-pET28a and Bl groups, respectively. A barplot analysis showing the thirteen most abundant phyla in the six groups are displayed in Fig. 4c. Consistent with the observations described above, *Bacteroidota* (*Bacteroidetes*) and *Bacillota* (*Firmicutes*) were the predominant phyla in the gut microbiota of all six groups. The relative abundances of *Bacteroidota* and *Bacillota* were respectively 74% and 16% in the control group, while their abundances were respectively 33% and 41% in the DSS group. In the Bl-cyp group, the abundances of *Bacteroidota* were significantly higher than those in the Bl group ($P < 0.001$), and the abundances of *Bacillota*

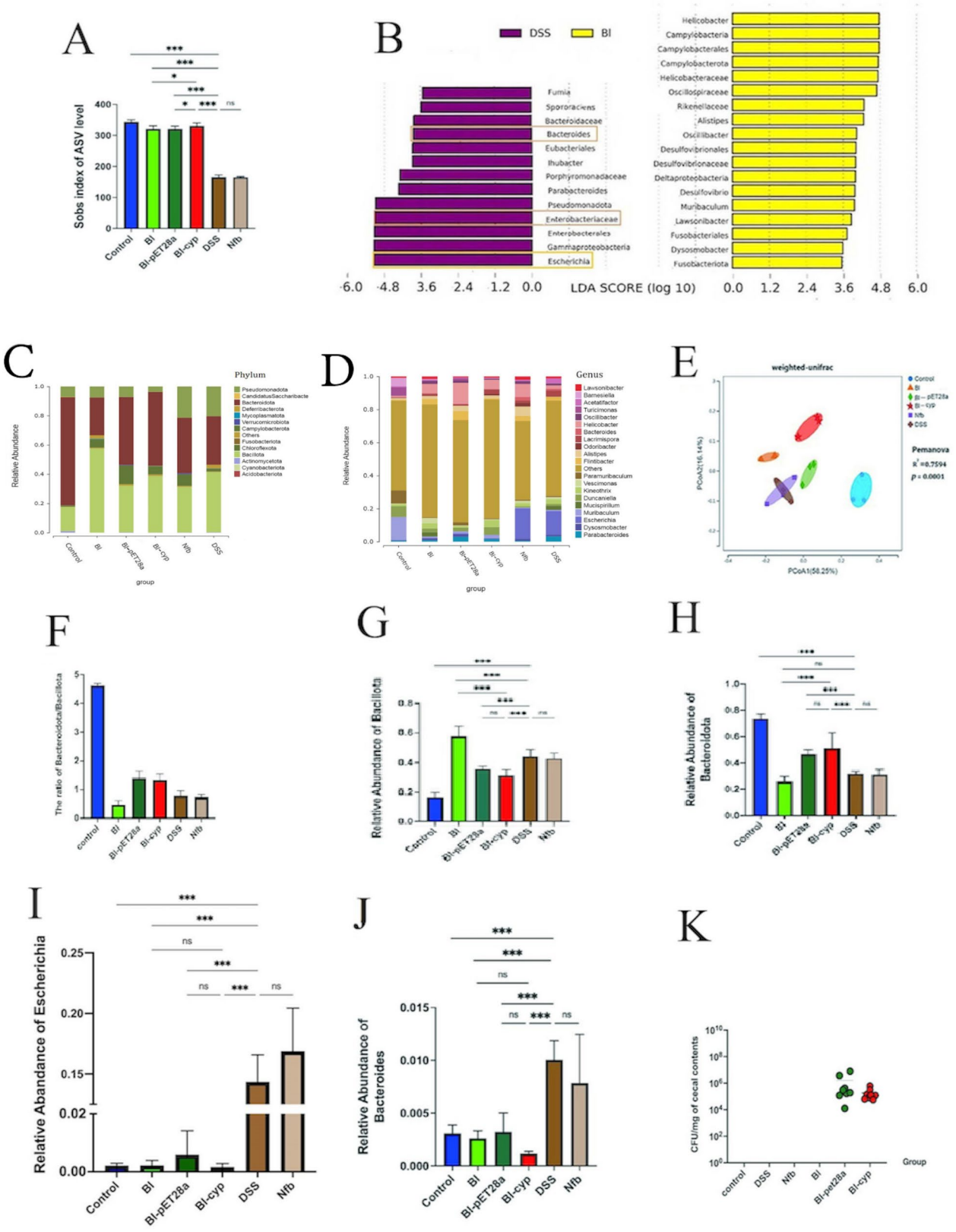

Fig. 4 (See legend on next page.)

(See figure on previous page.)

Fig. 4 Prophylactic administration of the Bl-cyp strain more effectively decreased DSS-induced gut microbiota disorder than other strains. **a** Comparison of the α-diversity of microbial communities in the DSS group with those in the control, Nfb, Bl, Bl-pET28a and Bl-cyp groups, and comparison of those in the Bl-cyp group with those in the Bl-pET28a and Bl groups by the Sobs index using a nonparametric test. **b** The differentially abundant taxa were determined from the linear discriminant analysis (LDA) scores (> 3.6) between the DSS (Brown) and Bl (Yellow) groups based on the Wilcoxon signed-rank test. The yellow frames represent *Bacteroides*, *Enterobacteriaceae* and *Escherichia* among the enriched taxa in the DSS group. **c** The relative abundance of microbial compositions in the six groups based on the barplot analysis (at the phylum level). **d** The relative abundance of microbial compositions in the six groups according to a barplot analysis (at the genus level). **e** Comparison of the β-diversity of microbial communities in the six groups was determined by a PCoA plot with a PERMANOVA analysis. **f** The ratios of *Bacteroidota*: *Bacillota* in the six groups are shown. **g** The commensal richness and diversity of *Bacillota* were compared in the six groups using a nonparametric test. **h** The commensal richness and diversity of *Bacteroidota* were compared in the six groups using a nonparametric test. **i** The commensal richness and diversity of *Escherichia* were compared in the six groups using a nonparametric test. **j** The commensal richness and diversity of *Bacteroides* were compared in the six groups with a nonparametric test. Data represent the means ± SD, $n = 3$ per group. * $P < 0.05$, ** $P < 0.01$, ***$P < 0.001$; NS, not significant. **k** The numbers of bacteria isolated from the fecal contents of mice with DSS-induced colitis that had been gavaged with cultures of the Bl, Bl-pET28a, or Bl-cyp strain, NS (control or DSS group) or medium (Nfb group)

were significantly lower than those in the Bl group ($P < 0.001$), while the abundances of both phyla were not significantly different from those in the Bl-pET28a group (Fig. 4g, h; $P = 0.163$; $P = 0.146$, respectively). Compared with the DSS group, the ratio of *Bacteroidota*: *Bacillota* showed an increasing trend in the Bl-cyp and Bl-pET28a groups, but not in the Bl group (Fig. 4f). The barplot in Fig. 4d showed the twenty most abundant genera in the six groups. The relative richness of *Escherichia* was significantly lower in all of the treatment groups, but not in the Nfb group, compared to the DSS group (all $P < 0.001$; $P = 0.103$). In addition, the richness in the Bl-cyp group was not significantly different from those in the Bl and Bl-pET28a groups (Fig. 4i; $P = 0.969$; $P = 0.77$, respectively). The relative richness of *Bacteroides* in the Bl-cyp group was significantly lower than those in the DSS group ($P < 0.001$), but not in the Bl and Bl-pET28a groups (Fig. 4j; $P = 0.267$ and $P = 0.115$). Therefore, these results indicate that the prophylactic administration of Bl-cyp strain enhanced the ratio of *Bacteroidota*: *Bacillota* more than the Bl strain, and also inhibited the excessive growth of opportunistic pathogen *Escherichia* just like the Bl or Bl-pET82a strain. It effectively regulated the disordered gut microbiota by improving their diversity, richness and compositions more than the Bl or Bl-pET82a strain.

Lastly, we isolated the Bl-pET28a and Bl-cyp strains (about 1×10^6 CFU/mg in Nfb with kanamycin) from the feces in the Bl-pET28a and Bl-cyp groups to confirm that these strains survived in the gut for some time. These strains were indeed culturable from feces, and the Bl-pET28a and Bl-cyp strains were not found in the control, Bl, DSS or Nfb group, confirming that the bacteria cultured from feces were indeed from the strains administered (Fig. 4k).

Prophylactic administration of the Bl-cyp strain decreased the DSS-induced colitis similar to the high concentration of ABA standard

Although ABA has been reported to effectively prevent IBD [21, 22], we wanted to confirm that it was effective in our model. We therefore investigated the effects of different concentrations of ABA standard in mice with DSS-induced colitis (Fig. 5a). The weights loss and increased DAIs in the ABA-high concentration (ABA-H) and ABA-low concentration (ABA-L) groups were significantly lower than those in the DSS group (Fig. 5b, c; all $P < 0.001$). The colon lengths of the mice in the DSS group were significantly shorter than those in the ABA-H group ($P = 0.007$), but were not significantly different from those in the ABA-L group (Fig. 5d, e; $P = 0.325$). The levels of IL-6 protein expression in the colon tissues of the DSS group were significantly higher than those in the ABA-H group ($P < 0.001$), but not in the ABA-L group (Fig. 5f; $P = 0.051$). The ABA-H group exhibited stronger protection of colon structures and less inflammation than the ABA-L group (Fig. 5g). The cumulative scores of each group were compared, and the results (Fig. 5h) were consistent with those shown in Fig. 5g. Therefore, the prophylactic administration of the high concentration of ABA standard contributed to decreased DSS-induced colitis. The low concentration of ABA standard did not have a significant effect on the colon inflammation.

Next, we compared the effects of treatment with the Bl-cyp strain in DSS-induced colitis to treatment with the ABA-H standard. The weights loss and increased DAIs in the Bl-cyp group were similar to those in the ABA-H group (Fig. 5b, c; $P = 0.9484$, $P = 0.9937$). The Bl-cyp group had longer colon lengths compared to the ABA-H group, but the difference was not statistically significant (Fig. 5d, e; $P = 0.091$). The protection of colon structures and IL-6 production in the Bl-cyp group were also similar to those in the ABA-H group (Fig. 5f, h; $P = 0.089$; $P = 0.589$, respectively). Therefore, the prophylactic administration of the Bl-cyp strain culture decreased DSS-induced colitis similar to the administration of the high concentration of ABA standard.

Comparison of the possible mechanisms of the action for the prophylactic administration of the Bl-cyp strain and the ABA-H standard

Exposure to ABA has been shown to regulate adhesion molecule expression through a PPAR-dependent mechanism, and is a regulator of the differentiation of Th17 and Treg cells [24]. We therefore compared the Th17/Treg

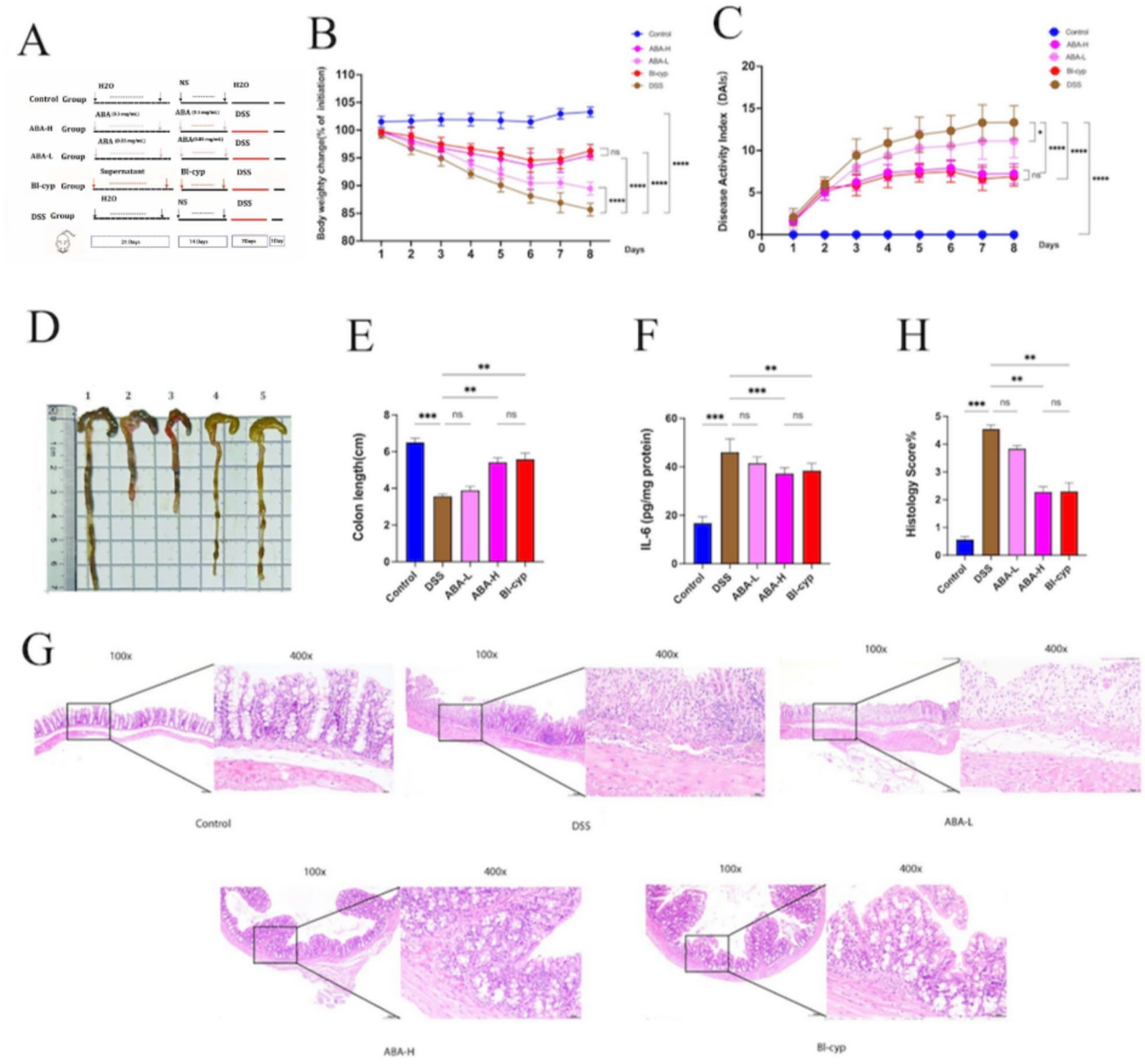

Fig. 5 Prophylactic administration of the Bl-cyp and ABA-H improved the colon inflammation in mice with colitis. **a** The experimental animal models in the control, Bl-cyp, ABA-H, ABA-L and DSS groups of mice with DSS-induced colitis. **b** The mouse body weights were recorded beginning the day after DSS was added to the drinking water. **c** The DAIs were recorded beginning on the day after DSS was added to the drinking water, and were based on the body weight loss and rectal bleeding and diarrhea. **d** The entire colons in the five groups were harvested on Day 43. The numbers 1–5 represent the colon lengths in the control, DSS, ABA-L, ABA-H and Bl-cyp groups, respectively. **e** Comparison of the colon lengths in the DSS group with those in the control, Bl-cyp, ABA-H and ABA-L groups, and comparison of those in the Bl-cyp with those in the ABA-H group. **f** Comparison of the IL-6 protein expression in the colon tissues of the DSS group with those in the control, Bl-cyp, ABA-H and ABA-L groups, and comparison of those in the Bl-cyp with those in the ABA-H. **g** Representative pictures of the H&E-stained colon tissues from the five groups were evaluated (scale bars,100 μm; magnification, 100x or 400x). **h** Comparison of the cumulative histology scores of colon tissues from the DSS group with those in the control, Bl-cyp, ABA-H and ABA-L groups, and comparison of those in the Bl-cyp with those in the ABA-H group. Data represent the means ± SD, $n = 6$–8 per group. Statistical significance was assessed using a one-way ANOVA, followed by Tukey's test. *$P < 0.05$, ** $P < 0.01$, *** $P < 0.001$; NS, not significant

balance in the ABA-H group with that in the Bl-cyp group in mice with DSS-induced colitis. First, we assessed the expression levels of pro-inflammatory and anti-inflammatory cytokines in the colon tissues. The results in both the Bl-cyp and ABA-H groups showed that the expression levels of Th17-type cytokines, TNF-α ($P = 0.005$ and $P = 0.002$) and IL-6 ($P = 0.004$ and $P = 0.001$), and a Th22-type cytokine, IL-22 ($P = 0.004$ and $P = 0.002$), significantly decreased following treatment compared to the DSS group. Conversely, the expression of a Treg-type cytokine, IL-10 ($P = 0.008$ and $P = 0.003$), significantly increased compared to the DSS group (Fig. 6a). However,

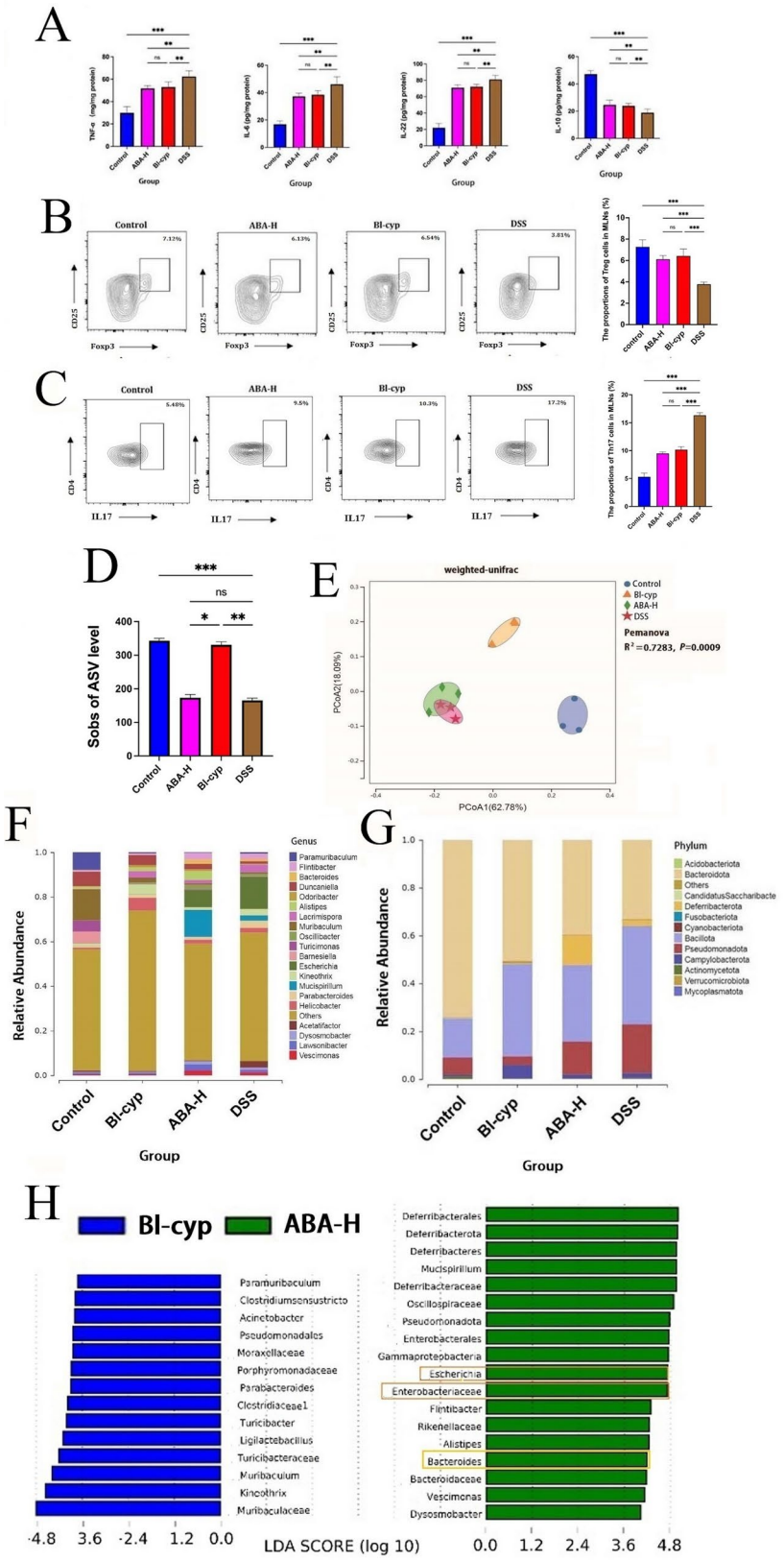

Fig. 6 (See legend on next page.)

(See figure on previous page.)

Fig. 6 Prophylactic administration of the Bl-cyp and ABA-H modulated immunity and microbiota in mice with colitis. **a** Concentrations of pro-inflammatory cytokines (TNF-a, IL-6, IL-22) and an anti-inflammatory cytokine (IL-10) in the colon tissues of the control, DSS, Bl-cyp and ABA-H groups. **b-c** The proportions of Treg ($CD45^+CD4^+CD25^+foxp3^+$) cells **(b)** and Th17 (CD45 + CD4 + IL-17 + foxp3-) cells **(c)** in murine mesenteric lymph nodes (MLNs) in the four groups were detected by flow cytometry. Data represent the means ± SD, $n = 6$–8 per group. Statistical significance was assessed using a one-way ANOVA, followed by Tukey's test. *$P < 0.05$, ** $P < 0.01$, *** $P < 0.001$; NS, not significant. **d** Comparison of the α-diversity of microbial communities in the DSS group with those in the control, ABA-H and Bl-cyp groups by a Sobs index with a nonparametric test. Data represent the means ± SD, $n = 3$ per group. * $P < 0.05$, ** $P < 0.01$, ***$P < 0.001$; NS, not significant. **e** Comparison of the β-diversity of microbial communities in the four groups by a PCoA plot with a PERMANOVA analysis. **f-g** The relative abundance of microbial compositions in the four groups based on barplot analyses at the phylum **(f)** and genus **(g)** levels. **h** The differentially abundant taxa identified from the linear discriminant analysis (LDA) scores (> 3.6) of the ABA-H (Green) and Bl-cyp (Blue) groups (from phylum to genus), based on the Wilcoxon signed-rank test. The yellow frames represent enriched taxa (*Bacteroides*, *Enterobacteriaceae* and *Escherichia*) in the ABA-H group

there were no obvious differences between these cytokines in the Bl-cyp and ABA-H groups (Fig. 6a; $P = 0.685$; $P = 0.608$; $P = 0.658$; $P = 0.681$, respectively).

Subsequently, we examined the frequencies of Th17 cells in mesenteric lymph nodes (MLNs), which induce immune hyperresponsiveness and promote inflammatory responses, and the frequencies of Treg cells, which play a key role in immune suppression [25]. The results showed that the proportion of lymphocytic subset Treg ($CD45^+CD4^+CD25^+Foxp3^+$) cells in the DSS group was significantly lower than that in the control group (Fig. 6b; $P < 0.001$), while the proportion of lymphocytic subset Th17 ($CD45^+CD4^+IL\text{-}17^+Foxp3^-$) cells in the DSS group was significantly higher than that in the control group (Fig. 6c; $P < 0.001$). Compared with the DSS group, the proportion of Treg cells were significantly decreased (Fig. 6b; all $P < 0.001$), and that of Th17 cells were increased in the Bl-cyp and ABA-H groups (Fig. 6c; all $P < 0.001$). However, there were no obvious differences in either the Th17 or Treg cells between the Bl-cyp and ABA-H groups (Fig. 6b, c; $P = 0.056$; $P = 0.392$, respectively). Therefore, these results suggested that prophylactic administration of both the ABA-H standard and the Bl-cyp strain could modulate the proportions of Treg and Th17 cells to suppress excessive gut inflammation in mice with DSS-induced colitis.

Next, we compared the effects of the administering the Bl-cyp strain versus the ABA-H standard on the gut microbiota in mice with colitis. The ASV level of the Sobs index in the Bl-cyp group was significantly higher than those in the ABA-H and DSS groups ($P = 0.0413$ and $P = 0.005$), but the ASV level in the ABA-H group was not significantly different from that in the DSS group (Fig. 6d; $P = 0.49$). The PCoA analysis showed statistically significant separations among the gut microbiota in the control, Bl-cyp, ABA-H and DSS groups (Fig. 6e; $R^2 = 0.7283$, $P = 0.0009$). However, while there was a clear separation between the Bl-cyp and DSS groups, but there was not a clear difference between the ABA-H and DSS groups. The barplots showing the twenty most abundant genera and twelve most abundant phyla in the four groups appear in Fig. 6f, g. The results revealed that the gut microbiota in the Bl-cyp group were different from those in the ABA-H group.

Next, to investigate the differences between the taxonomic compositions of the gut microbiota in the Bl-cyp and ABA-H groups, we performed LDA to identify differentially abundant biomarkers from the phylum to genus levels (indicated by a score > 3.6; Fig. 6h). The results showed that *Escherichia*, *Enterobacteriaceae* and *Bacteroides* were taxa more enriched in the ABA-H group, similar to the composition of gut microbiota in the DSS group, which differed from the Bl-cyp group. These results suggest that the administration of the Bl-cyp strain more effectively improved the gut microbiota than the ABA-H standard in mice with DSS-induced colitis. As such, the administration of the Bl-cyp strain could both modulate the immune response and decrease DSS-induced disorder of the gut microbiota.

Discussion

The gut is a complicated ecosystem consisting of resident microbiota, mucus layer, intestinal epithelium and immune cells. A well-established experimental models involving this complex gut ecosystem is DSS-induced colitis in mice [33]. DSS gradually injures intestinal epithelial cells, increasing the intestinal permeability, resulting in bacteria and antigens entering the mucous layer and activating inflammatory responses. In our study, the model with DSS-induced acute colitis was successfully established, as evidenced by severe inflammatory symptoms, colonic epithelial barrier damage and dysbiosis of the gut microbiota. This dysbiosis may be due to the presence of increased oxygen in the inflamed guts, which leads to an increase in the proportion of facultative anaerobes and obligate aerobes [34]. Our results demonstrated enrichment in *Enterobacteriaceae* and *Escherichia* in the DSS group, which are facultative anaerobes and opportunistic pathogens. In addition, our results showed that the ratio of *Bacteroidota (Bacteroidetes)*: *Bacillota* (*Firmicutes*) in the DSS group had a decreasing trend compared with the control group (Fig. 4h). The ratio of *Bacteroidetes*: *Firmicutes* is widely considered to play an important role in maintaining the homeostasis of gut microbiota. An increase or decrease in the ratio

is considered to indicate dysbiosis [35]. Our results also indicated that the relative richness of *Bacteroides* in the DSS group significantly increased compared with the control group. *Bacteroides fragilis* overgrowth is also known to be associated with the release of carcinogenic and pro-inflammatory factors, resulting in IBD and colorectal cancer [36].

The Bl strain is an obligate aerobe that consumes oxygen to regulate the gut microbiota and secretes digestive enzymes to promote the absorption of nutrients, and to enhance host immunity [11, 37]. Treatment with the Bl strain increases the expression of junction proteins in mice with DSS-induced colitis [13]. Recently, some reports suggested that Bl produces high levels of isobutyric acid and isovaleric acid in the gut, which are branched SCFAs that alleviate the inflammatory response to contribute to intestinal epithelial healing [12]. These products of the Bl strain increased the expression of the *occludin* gene and improved intestinal barrier function [37]. In the present study, the prophylactic administration of the Bl strain enhanced the expression of *occludin* mRNA and increased number of goblet cells in the gut, leading to decreased epithelial barrier damage, which was reflected by the lower serum LPS levels. The mucus layer protects epithelial cells from harmful factors, and is thus considered to reflect a function of the gut barrier [30]. Moreover, it has been reported that the administration of the Bl strain inhibited pathogenic adhesion [29] and modulated the gut microbiota in mice with DSS-induced colitis [13].

The gut microbiota is regarded as a major factor that controls the immune response [5]. Our results showed that the administration of the Bl and Bl-cyp strains could reduce the DSS-induced disorder of the microbiota by improving the commensal richness, diversity and composition of the microbes. The Bl supplementation could improve the bacterial composition by inhibiting the excessive growth of opportunistic *Escherichia*. The prophylactic administration of the Bl-cyp strain more effectively modulated the gut microbiota than supplementation with the Bl and Bl-pET28a strains. Interestingly, compared with the DSS group, the ratio of *Bacteroidota*: *Bacillota* showed an increasing trend in the Bl-cyp group, and a decreasing trend in the Bl group. The Bl strain belongs to the *Bacillota*, so supplementation would be expected to lead to an increase in the *Bacillota*. Therefore, the persistently high ratio in the Bl-cyp group was a surprising observation that warrants further evaluation in future studies.

It has been reported that the Bl strain reduced the production of pro-inflammatory IL-6 and reactive oxygen species by porcine intestinal epithelial cells [29]. In the present study, we similarly found that the administration of the Bl strain could reduce IL-6 expression in the colon tissues, resulting in attenuated inflammation in the gut.

The present study also showed that the Bl-cyp strain produced more ABA than the Bl and Bl-pET28a strains. Guri et al. suggested that prophylactic administration of ABA to mice in their diet for 35 days could modulate the T-cell populations and adhesion molecule expression and reduce leukocyte infiltration and gut inflammation [22]. They also proposed that the prophylactic administration could enhance the accumulation $Treg^+$ cells to ameliorate UC via a PPAR-dependent mechanism [23]. $Treg^+$ cells play a key role in immune suppression via IL-10 secretion and are essential to controlling the inflammatory responses in IBD [26, 38]. In our study, the administration of the Bl-cyp strain had similar effects on the immune response as the ABA-H standard, with an increased proportion of Treg $^+$ cells in MLNs and increased levels of IL-10 in the colon tissues, as well as a decreased proportion of Th17 cells. Uncontrolled activation of Th17 cells is closely associated with inflammation. Thus, the Bl-cyp strain could enhance immunity just like the Bl strain, but with more potent efficacy. It should be noted that the ABA standard used in this study was a mixture of (S)- (+)-ABA and (R)- (-)-ABA. The (S)-(+)-ABA, which is the natural compound produced by bacteria, has higher biological activity [39]. Since the Bl-cyp strain was able to be retained in the gut like the probiotic Bl strain [10], the application of the Bl-cyp strain could inhibit the excessive growth of opportunistic *Escherichia*.

In our study, we gavaged the mice with bacterial cultures, which had not been washed with phosphate buffer saline (PBS). We based the administration of a previous report by De Lacerda et al., where mice were gavaged with the bacterial cultures of a LLHsp65 strain overexpressing mycobacterial heat shock protein from *Lactococcus lactis*, which attenuated allergic asthma in their mouse model [40]. However, the expression of the *cyp* gene is unstable due to the loss of plasmids in the absence of the antibiotic, which may have reduced the activity in some cases (Fig. S6). In addition, as the Bl-cyp strain expressing the *cyp* in the pET28a-cyp plasmid exhibits antibiotic resistance, it is unsuitable for administration to humans. A balanced-lethal system was developed as an antigen gene carrier in *Listeria monocytogenes*, where a recombinant plasmid not requiring antibiotic selection carrying a housekeeping gene was transformed into a nutrient-deficient strain [41]. Such an approach could be developed for the Bl-cyp strain.

Conclusions

Together, the data from the present study suggest that the Bl-cyp strain could decrease the disorder of gut microbiota similar to (but more potently than) the Bl strain and could modulate the immune response like ABA, resulting

Table 1 Bacterial strains and plasmids used in the study

Strains or plasmids	Description and/or genotype	Source
Strains		
Bl	*Bacillus licheniformis* strain ATCC 12,759, wild type, origin, soil	RuiChu Company
Bl-pET28a	*B. licheniformis* strain ATCC 12,759 containing expression plasmid pET28a$^+$; Kan^r	This study
Bl-cyp	*B. licheniformis* strain ATCC 12,759 containing expression plasmid pET28a-cyp; Kan^r	This study
DH5α	*E. coil*; F-, ϕ80d/LacZM15, deoR△, recA1, endA, hsdR17, phoA, upE44, λs-, thi-1, gyrA96, relA1	SanYing Company
BL21	E. *coil*; F-, lon-11, Δ(ompT-nfrA) 885, Δ(galM-ybhJ)884	This study
Plasmids		
pET28a$^+$	origin, F1 vector, promoter T7, expression plasmid; Kan^r	Novagen Company
pET28a-cyp	1221 bp DNA fragment encompassing the cyp cloned into pET28a; Kan^r	This study

Table 2 Gene names and product sizes for qRT-PCR or PCR

Gene name	Primer sequence(5′-3′)	Product size (bp)	Methods
cyp	F: TATTGCTTGCCGCCACAGAACC R: GCGTCTCTGCGATTGCCTGAG	132	qRT-PCR
16SrRNA	F: GTAGTCCACGCTGTAAACGA R: GAATTAAACCACATGCTCCA	173	qRT-PCR
cyp	F: CCGGAATTCCGGAGCGGAC-GAAAGGGTGGAAT R: GGCGAGCTCGCCCTGGCGAAGATCAGT-GAGGC	1221	PCR
GAPDH	F: ACCCAGAAGACTGTGGATGG R: ACACATTGGGGGTAGGAACA	146	qRT-PCR
IL-6	F: TTTCCTCTGGTCTTCTGGAG R: CTGAAGGACTCTGGCTTTGT	92	qRT-PCR
occludin	F: TTGAAAGTCCACCTCCTTACAGA R: CCGGATAAAAAGAGTACGCTGG	184	qRT-PCR

F: forward primer, R: reverse primer

in reduced DSS-induced colitis. These findings suggest that a Bl-cyp-based approach may represent a new prevention strategy for IBD.

Methods

Bacterial strains, media and plasmids

The Bl strain ATCC 12,759 was purchased from RuiChu Company (Nanjing, China). The bacteria strains shown in Table 1 were cultivated in LB or Nfb medium. The plasmids used in the study are also listed in Table 1.

Cloning the *cyp* gene

The *cyp* gene primers in Table 2 were designed based on the genomic sequence of Bl strain ATCC14580 (GenBank accession number: NC_006270.3). A 1221 bp *cyp* fragment was amplified from Bl strain ATCC 12,759 by PCR and has been sequenced (GenBank accession number: 24077840). The *cyp* fragment was purified and ligated into a pET28a vector to produce a recombinant plasmid, pET28a-cyp (Fig. S1). The recombinant plasmid and control vector (pET28a) were separately transformed into *E.coli* BL21 by the $CaCl_2$ method. The pET28a-cyp/BL21 and pET28a/BL21 strains were obtained in LB plates (containing 100 μg/mL kanamycin). The plasmid pET28a-cyp and vector pET28a were separately introduced into the Bl strain ATCC 12,759 by electrotransformation [42]. The transformants, Bl-cyp and Bl-pET28a, were screened on LB (100 μg/mL kanamycin) plates.

Detection of the cyp expression in *E. coli* BL21 by SDS-PAGE

The pET28a-cyp/BL21 and the controls, pET28a/BL21 and BL21, were cultured in 5 mL LB (with or without 100 μg/mL kanamycin, as appropriate) medium at 37 °C overnight. After these cultures were transferred into fresh LB (with or without 100 μg/mL kanamycin) medium at a 1:100 ratio and cultivated for 2 h, 0.1, 0.2, 0.3 or 0.4 mM IPTG was added, and cultures were incubated at 37, 35, 33 or 31 ℃ for 4–2 h to induce to expression of the Cyp protein as has been described [43]. The cultures were then centrifuged at 12,000 g at 4 °C for 15 min, and the protein contents in the supernatants were determined using a bicinchoninic acid (BCA) protein assay kit (Beyotime Biotech Co., Ltd. Shanghai, China). Proteins in the supernatants were separated by 12% SDS-PAGE, and the gels were stained with Coomassie brilliant blue.

Identification of the ABA in supernatants by liquid chromatography-mass spectrometry (LC-MS)

Fresh Bl culture was transferred at 1:100 into 200 mL Nfb or LB medium, and was incubated at 37 °C for 48 h. After bacterial cultures were centrifuged at 12,000 rpm at 4 °C for 20 min, the supernatants were collected and sent to the SL Intelligent Analysis Testing Center (Nanjing Anteng LAN New Energy Co., LTD, Nanjing, China). The UPLC-Q-TOF-MS analysis was done using a Waters Xevo G2-XS Q-TOF system coupled to a Waters I-Class UPLC system (Waters Corporation, USA) with an electrospray source and spray interface (ESI) mode. Chromatographic separation was obtained using a Waters Acquity UPLC BEHC 18 column (2.1 mm × 100 mm, 1.7 μm) at 40℃. The mobile phase was made up of 0.1% formic acid in water (solvent A) and acetonitrile (solvent B) at a flow rate of 0.3 mL/min. The gradient elution procedures were as follows: 0–2 min, 90% A, 10% B; 2–8 min, 90% A, 10% B; 8–11 min, 10% A, 90% B; 11–20 min, 10%

A, 90% B; 20–25 min, 90% A, 10% B; 25–30 min, 90% A; 10% B. The injection volume was 1 μL.

The mass spectrometry was performed in the positive mode under a capillary voltage of 2.5 kV. For MS/MS studies, argon was used as the collision gas for the mass experiment, while the cone gas used nitrogen at a flow rate at 50 L/h. The desolvation gas flow was 600 L/h, and the source temperature was 120℃. Compounds were inspected by MS E centroid analysis with 0.5 s scans at a 30,000 resolving rate. The mass range was 100 to 1200 Da. An ABA standard solution (1 mg/mL, Sigma-Aldrich, Germany) was prepared as a quantitation control.

Detection of the ABA concentrations in the supernatants by ELISA

While the Bl, Bl-pET28a or Bl-cyp strain was growing in 200 mL Nfb (with or without 100 μg/mL kanamycin) at 37 °C, one milliliter of bacterial culture was taken out and centrifuged at different time points (12, 24, 48, 60, 72, 84–96 h), and the supernatants were collected. An ABA standard curve showing the relationship between a different concentrations of ABA standard and the corresponding spectrophotometric absorbances (OD_{450}) was generated. ABA was detected using an ELISA kit (Sailuofei Biotech Co., Ltd., Wuhan, China) as described in the manufacturer's instructions. In brief, ten microliters of bacterial supernatant was added to forty microliters of diluent and fifty microliters of enzyme-labeled reagent in a well of a 96-well plate, then the mixture was incubated at 37 °C for 30 min, and one hundred microliters of color-developing reagent was added to the mixture. The absorbance at OD_{450} was measured for at least two dilutions using a microplate reader, and the relative ABA concentrations were calculated from the ABA standard curve.

Establishment of mice with DSS-induced colitis

Six-week-old female C578L/6 mice weighing between 18 and 22 g were used for the study and were obtained from the Experimental Animal Center of Yangzhou University. The mouse grouping was designed according to the ARRIVE guidelines 2.0 [33, 44]. After 7 d of acclimation under specific pathogen-free conditions at the experimental animal center of the Medicine School of Southeast University, mice were randomly divided into control, DSS, Nfb, Bl, ABA-H, ABA-L, Bl-pET28a and Bl-cyp groups. The mice in the Nfb, Bl, Bl-pET28a and Bl-cyp groups were respectively fed with control Nfb medium or supernatant from Bl, Bl-pET28a, or Bl-cyp bacteria cultured for 48 h in 5 mL Nfb (with or without 100 μg/mL kanamycin) at 37 °C for 21 d. For those administered the supernatants, the cultures were first centrifuged at 3000 g for 10 min, then the supernatants were separated. The mice in the ABA-H, ABA-L, DSS and control groups were administered distilled water with or without ABA (0.5 for the High (H) group or 0.05 mg/mL for the Low (L) group) for 21 d. Then, the mice in the control and DSS-only groups received a daily gavage with normal saline (NS) for 14 d, while the mice in the other groups received daily oral gavage treatments with 200 μL bacterial cultures from the Bl, Bl-pET28a or Bl-cyp strain (3×10^8 CFU/mL), ABA solution (0.5 or 0.05 mg/mL), or Nfb medium for 14 d, followed by daily oral administration of 2.5% (w/v) DSS (Aladdin Company, Shanghai, China) in distilled water for 7 d. All mice were administered distilled water the day before sacrifice.

Sample collection and preservation

During all experiments, the body weight and DAIs in the eight groups of mice were recorded after the administration of 2.5% DSS at the same time every day. The DAIs were used to assess the severity of colitis by combining body weight loss and fecal diarrhea with blood content in the feces [45].

Mice in all groups were anaesthetized and kept unconscious with anesthetic isoflurane using a small animal anesthesia machine (RWD Life Science Co., LTD, Shenzhen, China) before sacrifice on Day 43. Mice inhaled 4–5% isoflurane to induce anesthesia, then 1.5-2% isoflurane was used to maintain animal anesthesia, then mice were killed by cervical dislocation. Blood was then collected from the retroorbital sinus into a 1.5 mL tube and was stored at 4 °C overnight. The plasma was obtained after 2000 rpm centrifugation for 15 min and was kept at -20 °C. The MLNs were excised, crushed and resuspended in sterile NS at 4 °C.

After the colons were excised, their lengths were measured. Some colon tissues were fixed in 4% paraformaldehyde, and approximately 100 mg of fresh colon tissue and colonic fecal content from each mouse were preserved at -70 °C. The other colonic fecal contents were stored at 4 °C.

Bacterial isolation from the colonic fecal contents of mice

To assess the colonization of the administered Bl-pET28a and Bl-cyp strains, the colon contents from mice were resuspended in sterile normal saline (NS), diluted and incubated on Nfb (with 100 μg/mL kanamycin) plates at 37 °C to calculate the bacterial CFUs/mg of colonic fecal contents.

RNA isolation and quantitative real-time PCR (qRT-PCR)

After the Bl, Bl-cyp, or Bl-pET28a strains were cultured in 1 mL Nfb medium (with or without 100 μg/mL kanamycin) at 37 °C for 48 h, the contents were centrifuged at 12,000 rpm for 15 min, then the cells pellets were treated with TRIzol reagent (TaKaRa, Dalian, China). An approximately 100 mg colon tissue specimen from each mouse was taken out from the − 70 °C freezer, washed

in diethyl pyrocarbonate (DEPC) water and homogenized after TRIzol treatment. Total RNA was reverse-transcribed using a PrimeScript™ RT reagent kit (Takara, Dalian, China). Then, qRT-PCR was done using the primers listed in Table 2 and SYBR Premix Ex Taq (Takara, Dalian, China) in an ABI 7300 real-time detection system (Applied Bio-systems Company, USA). The relative mRNA levels of the *cyp* gene in the Bl-pET28a and Bl strains were compared with that in the Bl-cyp strain by the 2 -△△CT method [46]. The bacterial 16 S rRNA gene was used as a quantitation control. The relative mRNA levels of the genes encoding IL-6 and Occludin in the colon tissues of mice were determined using the GAPDH gene as a control.

Detection the proportions of Treg and Th17 cells by flow cytometry analysis

As described in the manufacturer's instructions (Biolegend, USA), the MLNs were placed in a filter (100 mm) and ground evenly until lymphocytes were fully dispersed. The MLN-derived cells were resuspended in 1 mL PBS and centrifuged at 500 g for 4 min, then were incubated with a fixable viability stain (Invitrogen, USA) for live cell staining, and Alexa Fluor 700 anti-mouse CD45, APC anti-mouse CD4 and PerCp anti-mouse CD25 (Biolegend, USA) for cell surface staining for 30 min at room temperature away from light. Next, the cells were permeabilized with Biolegend fixation buffer (Biolegend, USA) and incubated with Alexa 488 anti-mouse Foxp3 and Efluor 450 anti-mouse IL-17 (Biolegend, USA) for intracellular staining at room temperature for 45 min. Sample staining was assessed using an AttuneTM NxT Flow Cytometer (Thermo, USA). The results was analyzed with FlowJo software (Tree Star Inc., San Carlos, USA). Th17 cells were identified as the $CD45^+$ $CD4^+$ $IL\text{-}17^+Foxp3^-$ population and Treg cells were identified as the $CD45^+CD4^+$ $CD25^+$ $Foxp3^+$ population.

Detection of inflammatory cytokines in the colon tissues by ELISA

Samples of frozen colon tissues were homogenized and digested with a protease inhibitor (Solarbio, China). After the homogenates were centrifuged at 12,000 rpm at 4 °C for 15 min, the protein contents in the supernatants were inspected using a BCA protein assay kit (Beyotime Biotech Co., Ltd. Shanghai, China), and the concentrations of pro-inflammatory cytokines (TNF-α, IL-6 and IL-22), and an anti-inflammatory cytokine (IL-10) in colon tissues were detected in triplicate using an ELISA kit (Table S1; Nanjing Lapuda Biotechnology Co., Ltd., Nanjing, China).

Histological analysis

Tissue samples were fixed in 4% paraformaldehyde, embedded in paraffin and sectioned (5 μm thick). Sections stained with hematoxylin and eosin (H&E) were scored for histopathological analysis on the basis of the extent of inflammatory cell infiltration (0–5), ulceration (0–3), crypt damage (0–4) and edema (0 or 1) [47]. Parameters were calculated and summed to obtain total scores.

Immunofluorescence staining to count the number of goblet cells

As described in the manufacturer's recommendations (ThermoFisher, USA), the main steps for immunofluorescence staining were: Repairing the antigen in sections was performed in a water bath at 95 °C for 20 min. The sections were permeabilized with 0.2% Triton for 20 min at room temperature, and blocked with 10% goat serum for 1 h. Then, the sections were incubated with antibodies against mouse epithelial cell marker (EpCAM, CD326) and goblet cell marker (MUC2) at room temperature for 1 h. Ten microliters of histology mounting medium including DAPI were dropped on a glass slide. A coverslip was used to cover the slide. Images were obtained using a confocal laser scanning microscope. The numbers of goblet cells and epithelial cells in the six groups were randomly measured in five spots per slice. The proportion of goblet cells/epithelial cells in the six groups was calculated as previously described by Fang et al. [48].

Limulus amebocyte lysate testing to detect LPS in sera

The sera were collected from mice using limulus amebocyte lysate to detect LPS, as described in the manufacturer's instructions (SunShine, Nanjing, China). A standard curve for LPS showing the relationship between a series of concentrations of a LPS standard and the corresponding OD_{450} values was established. The OD_{450} of serum LPS was measured for at least two dilutions in a microplate reader, and its relative concentration was calculated using the standard curve.

Fecal bacterial DNA extraction

The colonic fecal contents in mice had been frozen at -70 °C. These samples were delivered to BGI Genomics Co., Ltd (Shenzhen, China) for analysis. Bacterial DNA was extracted from the contents using the QIAGEN stool kit on the basis of the manufacturer's protocols (Qiagen, Germany). PCR amplification was used to amplify the V3-V4 region of bacterial 16 S ribosomal DNA with 16 S rRNA gene primers (Table 2) in a 20 μL reaction using Phusion Hot Start Flex 2X Master Mix (New England Biolabs, USA). The PCR product was extracted with AMPure XT Beads (Beckman Coulter Genomics, USA), and qualified with Qubit (Invitrogen, USA). The purity

and concentration of the DNA product was assessed using an Agilent 2100 Bioanalzyer (Asia gene, Shanghai, China).

Sequencing and analysis of microbiota

The DNA products were evaluated using an Illumina library quantitative kit (Kapa, Biosciences, USA), and were sequenced on an Illumina NovaSeq PE250 platform (Personalbio, Shanghai, China). De-multiplexed raw sequences were removed from the sequencing primer using software cutadapt (v1.9). The short reads (< 100 bp), low-quality reads (quality scores < 20), and more than 5% N reads were trimmed using fqtrim software (v 0.94). Then, paired-end reads were joined to obtain tags using FLASH software (v1.2.11). Chimeric sequences were filtered with Vsearch software (v2.3.4). Unique ASVs were generated and classified based on the presence of 100% sequence similarity using DATA2. The α-diversity and β-diversity analyses were performed according to the sequence features and abundances of ASVs. We applied the Sobs index, PCoA and permutational multivariate analysis of variance (PERMANOVA) based on Bray-Curtis distances to perform α-diversity and β-diversity analyses with QIIME2 (http://forum.qiime2.org) [49].

Statistical analysis

Data from at least 3 independent experiments are presented as the means ± standard deviation (SD) and were analyzed with the Graph Pad Prism 8.0 Program (Graph Pad Software San Diego, Canada). Data from at least two groups were assessed using a one-way analysis of variance (ANOVA), followed by Tukey's test. The β-diversity analyses (PCoA) were performed with a PERMANOVA test. The α-diversity analyses (Sobs) were performed with nonparametric tests. The results were considered to be significant at probability (*P*) values less than 0.05.

Supplementary Information

The online version contains supplementary material available at https://doi.org/10.1186/s12866-025-03988-4.

Supplementary Material 1

Acknowledgements

We are grateful to the staffs at the Public Scientific Research Platforms of the Department of Pathogenic Microbiology and Immunology of the Medicine School of Southeast University, and Zhongda Hospital Affiliated with Southeast University for technical assistance.

Author contributions

Z.X. wrote the main manuscript. L.Z. and Z.X. generated Figs. 1 and 6. M.W. and A.C. performed the experiments shown in Figs. 2 and 5. G.Z. and J.Z. performed the work shown in Fig. 3. Z.X. and W.C. generated Figure 4. D.G. and R.S. supervised the research. D.G. and R.S. acquired funding. All authors reviewed the manuscript.

Funding

This work was supported by Chinese National Nature and Science Foundation (Grant no.31570124) and a Project in Science and Education of Jiangsu Province (Grant no. 2017ZXK7QW08).

Data availability

Sequence data that support the findings of this study have been deposited in the NCBI with the accession ID PRJNA1131321.

Declarations

Ethics approval and consent to participate

These mice have been obtained from the Experimental Animal Center of Yangzhou University. The animal experiments were approved by the Ethics Committee of Experimental Animals of Southeast University (20230301020). All animal experiments were performed in according to the ARRIVE guidelines 2.0 [44].

Consent for publication

Not applicable.

Competing interests

The authors declare no competing interests.

Author details

[1]School of Medicine, Southeast University, Nanjing, Jiangsu 210009, China
[2]Department of Gastroenterology, Affiliated Zhongda Hospital, Southeast University, Nanjing, Jiangsu 210009, China

Received: 17 December 2024 / Accepted: 23 April 2025
Published online: 19 May 2025

References

1. Ramos GP, Papadakis KA. Mechanisms of disease: inflammatory bowel diseases. Mayo Clin Proc. 2019;94:155–65. https://doi.org/10.1016/j.mayocp.2018.09.013.
2. Kaplan GG. The global burden of IBD: from 2015 to 2025. Nat Rev Gastroenterol Hepatol. 2015;12:720–27. https://doi.org/10.1038/nrgastro.2015.150.
3. Wright EK, Ding NS, Niewiadomski O. Management of inflammatory bowel disease. Med J Aust. 2018;209:318–23. https://doi.org/10.5694/mja17.01001.
4. Hamamah S, Amin A, Al-Kassir AL, Chuang J, Covasa M. Dietary fat modulation of gut microbiota and impact on regulatory pathways controlling food intake. Nutrients. 2023;15:3365. https://doi.org/10.3390/nu15153365.
5. Knox NC, Forbes JD, Peterson C, Van Domselaar G, Bernstein CN. The gut Microbiome in inflammatory bowel disease: lessons learned from other Immune-Mediated inflammatory diseases. Am J Gastroenterol. 2019;114:1051–70. https://doi.org/10.14309/ajg.0000000000000305.
6. Morrison DJ, Preston T. Formation of short chain fatty acids by the gut microbiota and their impact on human metabolism. Gut Microbes. 2016;7:189–200. https://doi.org/10.1080/19490976.2015.1134082.
7. Shen ZH, Zhu CX, Quan YS, Yang ZY, Wu S, Luo WW, Tan B, Wang XY. Relationship between intestinal microbiota and ulcerative colitis: mechanisms and clinical application of probiotics and fecal microbiota transplantation. World J Gastroenterol. 2018;24:5–14. https://doi.org/10.3748/wjg.v24.i1.5.
8. Lavelle A, Sokol H. Gut Microbiota-derived metabolites as key actors in inflammatory bowel disease. Nat Rev Gastroenterol Hepatol. 2020;17:223–37. https://doi.org/10.1038/s41575-019-0258-z.
9. Amer M, Nadeem M, Nazir SUR, Fakhar M, Abid F, Ain QU, Asif E. Probiotics and their use in inflammatory bowel disease. Altern Ther Health Med. 2018;24:16–23.
10. Muras A, Romero M, Mayer C, Otero A. Biotechnological applications of *Bacillus licheniformis*. Crit Rev Biotechnol. 2021;41:609–27. https://doi.org/10.1080/07388551.2021.
11. Wu T. Biologic characteristics of Bacillus lichniformis strain 20386 and its Micro-ecologic activities in vitro and in vivo. Chin J Microecol. 1990;2:1–12.
12. Feng S, Meng C, Hao Z, Liu H. *Bacillus licheniformis* reshapes the gut microbiota to alleviate the subhealth. Nutrients. 2022;14:1642. https://doi.org/10.3390/nu14081642.

13. Li Y, Liu M, Zhou J, Hou B, Su X, Liu Z, Yuan J, Li M. *Bacillus licheniformis* Zhengchangsheng® attenuates DSS-induced colitis and modulates the gut microbiota in mice. Benef Microbes. 2019;10:543–53. https://doi.org/10.3920/BM2018.0122.
14. Heo J, Kim SK, Park KS, Jung HK, Kwon JG, Jang BIA, Double-Blind R, Comparative AD. Parallel-Group, Multi-Center clinical study to evaluate the safety and efficacy of probiotics (*Bacillus licheniformis*, Zhengchangsheng® capsule) in patients with diarrhea. Intest Res. 2014;12:236–44. https://doi.org/10.5217/ir.2014.12.3.236.
15. Salomon MV, Bottini R, de Souza Filho GA, Cohen AC, Moreno D, Gil M, Piccoli P. Bacteria isolated from roots and rhizosphere of Vitis vinifera retard water losses, induce abscisic acid accumulation and synthesis of defense-related terpenes in in vitro cultured grapevine. Physiol Plant. 2014;151:359–74. https://doi.org/10.1111/ppl.12117.
16. Nambara E, Marion-Poll A. Abscisic acid biosynthesis and catabolism. Annu Rev Plant Biol. 2005;56:165–85. https://doi.org/10.1146/annurev.arplant.56.032604.144046.
17. Magnone M, Sturla L, Guida L, Spinelli S, Begani G, Bruzzone S, Fresia C, Zocchi E. Abscisic Acid: A conserved hormone in plants and humans and a promising aid to combat prediabetes and the metabolic syndrome. Nutrients. 2020;12:1724. https://doi.org/10.3390/nu12061724.
18. Shi TQ, Peng H, Zeng SY, Ji RY, Shi K, Huang H, Ji XJ. Microbial production of plant hormones: opportunities and challenges. Bioengineered. 2017;8:124–28. https://doi.org/10.1080/21655979.2016.1212138.
19. Abdel-Hamid MS, Fouda A, El-Ela HKA, El-Ghamry AA, Hassan SE. Plant growth-promoting properties of bacterial endophytes isolated from roots of Thymus vulgaris L. and investigate their role as biofertilizers to enhance the essential oil contents. Biomol Concepts. 2021;12:175–96. https://doi.org/10.1515/bmc-2021-0019.
20. Nguyen CH, Yan D, Nambara E. Persistence of abscisic acid analogs in plants: chemical control of plant growth and physiology. Genes (Basel). 2023;14:1078. https://doi.org/10.3390/genes14051078.
21. Zhao CC, Xu J, Xie QM, Zhang HY, Fei GH, Wu HM. Abscisic acid suppresses the activation of NLRP3 inflammasome and oxidative stress in murine allergic airway inflammation. Phytother Res. 2021;35:3298–309. https://doi.org/10.1002/ptr.7051.
22. Guri AJ, Evans NP, Hontecillas R, Bassaganya-Riera JA. T cell PPAR gamma is required for the anti-inflammatory efficacy of abscisic acid against experimental ibd. J Nutr Biochem. 2011;22:812–19. https://doi.org/10.1016/j.jnutbio.2010.06.011.
23. Guri AJ, Hontecillas R, Bassaganya-Riera J. Abscisic acid ameliorates experimental IBD by down regulating cellular adhesion molecule expression and suppressing immune cell infiltration. Clin Nutr. 2010;29:824–31. https://doi.org/10.1016/j.clnu.2010.02.009.
24. Xu X, Wang Y, Wei Z, Wei W, Zhao P, Tong B, Xia Y, Dai Y. Madecassic acid, the contributor to the anti-colitis effect of madecassoside, enhances the shift of Th17 toward Treg cells via the PPARgamma/AMPK/ACC1 pathway. Cell Death Dis. 2017;8:e2723. https://doi.org/10.1038/cddis.2017.150.
25. Sha S, Zeng H, Gao H, Shi H, Quan X, Chen F, Liu M, Xu B, Liu X. Adherent-invasive *Escherichia coli* LF82 aggravated intestinal inflammation in colitis mice by affecting the gut microbiota and Th17/Treg cell differentiation balance. Arch Microbiol. 2023;205:218. https://doi.org/10.1007/s00203-023-03570-4.
26. Cho J, Kim S, Yang DH, Lee J, Park KW, Go J, Hyun C, Jee Y, Kang KS. Mucosal immunity related to FOXP3(+) regulatory T cells, Th17 cells and cytokines in pediatric inflammatory bowel disease. J Korean Med Sci. 2018;33:e33. https://doi.org/10.3346/jkms.2018.33.e336.
27. Karadeniz A, Topcuog˘lu SF, Inan S. Auxin, Gibberellin, cytokinin and abscisic acid production in some bacteria. World J Microbiol Biotechnol. 2006;22:1061–64.
28. Siewers V, Smedsgaard J, Tudzynski P. The P450 monooxygenase BcABA1 is essential for abscisic acid biosynthesis in *Botrytis cinerea*. Appl Environ Microbiol. 2004;70:3868–76. https://doi.org/10.1128/AEM.70.7.3868-3876.2004.
29. Palkovicsné Pézsa N, Kovács D, Rácz B, Farkas O. Effects of *Bacillus licheniformis* and *Bacillus subtilis* on gut barrier function, Proinflammatory response, ROS production and pathogen Inhibition properties in IPEC-J2-*Escherichia coli*/*Salmonella typhimurium* Co-Culture. Microorganisms. 2022;10:936. https://doi.org/10.3390/microorganisms10050936.
30. Pelaseyed T, Bergström JH, Gustafsson JK, Ermund A, Birchenough GM, Schütte A, van der Post S, Svensson F, Rodríguez-Piñeiro AM, Nyström EE, Wising C, Johansson ME, Hansson GC. The mucus and mucins of the goblet cells and enterocytes provide the first defense line of the Gastrointestinal tract and interact with the immune system. Immunol Rev. 2014;260:8–20. https://doi.org/10.1111/imr.12182.
31. Wu H, Xie S, Miao J, Li Y, Wang Z, Wang M, Yu Q. Lactobacillus reuteri maintains intestinal epithelial regeneration and repairs damaged intestinal mucosa. Gut Microbes. 2020;11:997–1014. https://doi.org/10.1080/19490976.2020.1734423.
32. Kuo WT, Odenwald MA, Turner JR, Zuo L. Tight junction proteins occludin and ZO-1 as regulators of epithelial proliferation and survival. Ann N Y Acad Sci. 2022;1514:21–33. https://doi.org/10.1111/nyas.14798.
33. Jurius A, Khoury NN, Reimund JM. Animal models of inflammatory bowel disease[J]. J Pharmacol Toxicolog Methods. 2004;50:81–92. https://doi.org/10.1016/j.vascn.2003.12.002.
34. Henson MAPP. Microbiota dysbiosis in inflammatory bowel diseases: in Silico investigation of the oxygen hypothesis. BMC Syst Biol. 2017;10:45. https://doi.org/10.1186/s12918-017-0522-1.
35. Stojanov S, Berlec A, Štrukelj B. The influence of probiotics on the *Firmicutes/Bacteroidetes* ratio in the treatment of obesity and inflammatory bowel disease. Microorganisms. 2020;8:1715. https://doi.org/10.3390/microorganisms8111715.
36. Cao Y, Wang Z, Yan Y, Ji L, He J, Xuan B, Shen C, Ma Y, Jiang S, Ma D, Tong T, Zhang X, Gao Z, Zhu X, Fang JY, Chen H, Hong J. Enterotoxigenic *Bacteroides fragilis* promotes intestinal inflammation and malignancy by inhibiting Exosome-Packaged miR-149-3p. Gastroenterology. 2021;161:1552–e156612. https://doi.org/10.1053/j.gastro.2021.08.003.
37. Chen YW, Yu YH. Differential effects of *Bacillus subtilis* and *Bacillus licheniformis*-fermented products on growth performance, intestinal morphology, intestinal antioxidant and barrier function gene expression, cecal microbiota community, and microbial carbohydrate-active enzyme composition in broilers. Poult Sci. 2023;102:102670. https://doi.org/10.1016/j.psj. 2023. 102670.
38. Fan L, Qi Y, Qu S, Chen X, Li A, Hendi M, Xu C, Wang L, Hou T, Si J, Chen S. *B.adolescentis* ameliorates chronic colitis by regulating Treg/Th2 response and gut microbiota remodeling. Gut Microbes. 2021;13:1–17. https://doi.org/10.1080/19490976.2020.1826746.
39. Shen JX, Niwan TMS. Comparison of the biological activity of natural (S)-(+)-ABA and Non-Nantural (R)-(-)-ABA. Acta Phytophysiol Sinia. 1995;21:15240257.
40. Lacerda LB, Rios WM, Masson AP, Brandão IT, Milani TM, Borges MC, Ramalho LNZ, Barbosa MCR, Miyoshi A, Silva CL. Oral administration of Hsp65-producing *Lactococcus lactis* attenuates allergic asthma in a murine model. J Appl Microbiol. 2021;130:2075–86. https://doi.org/10.1111/jam.14913.
41. Lei Y, Zhou Y, Zhang Y, Liu S, Tian S, Ou Q, Liu T, Huang H, Tang T, Wang C. *Listeria ivanovii* balanced-lethal system May be a promising antigen carrier for vaccine construction. Microb Biotechnol. 2022;15:2831–44. https://doi.org/10.1111/1751-7915.14137.
42. Welker DL, Hughes JE, Steele JL, Broadbent JR. High efficiency electrotransformation of *Lactobacillus casei*. FEMS Microbiol Lett. 2015;362:1–6. https://doi.org/10.1093/femsle/fnu033.
43. Gao D, Cheng J, Zheng E, Li Y, Shao Z, Xu Z, Lu C. Eha, a transcriptional regulator of hemolytic activity of Edwardsiella tarda. FEMS Microbiol Lett. 2014;353:132–40. https://doi.org/10.1111/1574-6968.12420.
44. Percie du Sert N, Hurst V, Ahluwalia A, Alam S, Avey MT, Baker M, Browne WJ, Clark A, Cuthill IC, Dirnagl U, et al. The ARRIVE guidelines 2.0: updated guidelines for reporting animal research. PLOS Biol. 2020;18:e3000410. https://doi.org/10.1371/journal.pbio.3000410.
45. Wu Z, Huang S, Li T, Li N, Han D, Zhang B, Xu ZZ, Zhang S, Pang J, Wang S, Zhang G, Zhao J, Wang J. Gut microbiota from green tea polyphenol-dosed mice improves intestinal epithelial homeostasis and ameliorates experimental colitis. Microbiome. 2021;9:184. https://doi.org/10.1186/s40168-021-01115-9.
46. Livak KJ, Schmittgen TD. Analysis of relative gene expression data using real-time quantitative PCR and the 2(-Delta Delta C(T)) method. Methods. 2001;25:402–8. https://doi.org/10.1006/meth.2001.1262.
47. Peng Y, Yan Y, Wan P, Chen D, Ding Y, Ran L, Mi J, Lu L, Zhang Z, Li X, Zeng X, Cao Y. Gut microbiota modulation and anti-inflammatory properties of anthocyanins from the fruits of Lycium ruthenicum Murray in dextran sodium sulfate-induced colitis in mice. Free Radic Biol Med. 2019;13696–108. https://doi.org/10.1016/j.freeradbiomed.2019.04.005.
48. Fang F, Liu Y, Xiong Y, Li X, Li G, Jiang Y, Hou X, Song J. Slowed Intestinal Transit Induced by Less Mucus in Intestinal Goblet Cell Piezo1-DeficientMice through Impaired Epithelial Homeostasis. Int J Mol Sci. 2023;24:14377–95. https://doi.org/10.3390/ijms241814377.

49. Bolyen E, Rideout JR, Dillon MR, Bokulich NA, Abnet CC, Al-Ghalith GA, Alexander H, Alm EJ, Arumugam M, Asnicar F, et al. Author correction: reproducible, interactive, scalable and extensible Microbiome data science using QIIME 2. Nat Biotechnol. 2019;37:1091. https://doi.org/10.1038/s41587-019-0252-6.

Publisher's note